

# Effect of Tuning the Structure on the Optical and Magnetic Properties by Various Transition Metal Doping in ZnO/TM (TM = Fe, FeCo, Cr, and Mn) Thin Films

A. El Haimeur<sup>1,2,3</sup>  · L. El Gana<sup>4</sup> · M. Addou<sup>1,2</sup> · A. El Kenz<sup>5</sup>

Received: 5 June 2017 / Accepted: 28 June 2017 / Published online: 24 July 2017  
© Springer Science+Business Media, LLC 2017

**Abstract** We have investigated in this work the physical, optical, electronic, and the magnetic behavior (Curie temperature, magnetic moment) of Zn<sub>1-x</sub>M<sub>x</sub>O (M = Fe 5%, Co 1%, Cr 5%, and Mn 5%), diluted magnetic semiconductors (DMSs). The samples were deposited on glass substrate by the spray pyrolysis technique, and the results of the x-ray diffraction (XRD) of the prepared substrates was used to prove the incorporation of the dopants into the ZnO lattice host; the ferromagnetic and the antiferromagnetic state competitions and their effects on the physical, magnetic, and optical properties, were investigated. The electronic structure and magnetic properties of transition metal (TM) defects, were investigated in detail, by using the Korringa–Kohn–Rostoker (KKR) method combined with the coherent

potential approximation (CPA). As a result, doping by TM impurities induce the ferromagnetism with different competitions between the ferromagnetic and antiferromagnetic states, which affects the physical properties of the TM (Fe, Fe/Co, Cr, and Mn)-doped ZnO, with a Curie temperature closer to room-temperature ferromagnetic.

**Keywords** Magnetism · Diluted magnetic semiconductors DMS · Akai KKR · Curie temperature · RTFM

## 1 Introduction

Diluted magnetic semiconductors have attracted many research groups [1–3]. However the diluted magnetic oxide (DMO) [2, 4, 5] are also used for manufacturing electrodes for magnetic junction (MTJ)-based materials [6, 7]. This is motivated by the large  $T_c$  [6, 8] and the high rate of TMR at 180 and 250 K. However the diluted magnetic semiconductors (DMSs) which used the ZnO as lattice host [9–11] where the metal-doped ZnO [12–14] was a good choice for the untotoxicity of the ZnO and other transition metals such as the Fe [14–16], Co [17–22], Cr [23–25], and Mn-doped ZnO [26–28].

The zinc oxide is a semiconductor with a large optical band gap with about 3.1–3.6 eV [29, 30], has very important magnetic and optical properties, which made these devices multifunctional materials. DMO is also used for manufacturing MTJ electrodes. However, ZnO doped by transition metal (TM) exhibits the room-temperature ferromagnetic (RTFM) and made it a candidate for spintronics applications [21, 31–33].

In this study, we investigate in the band structure and the electronic, magnetic, and optical properties of the TM (Fe, Fe/Co, Cr, Mn)-doped ZnO by combining between the

✉ A. El Haimeur  
elhaimeur.amine@gmail.com

<sup>1</sup> Laboratory of Materials and Valorization of Natural Resources, University Abdelmalek Essaadi-FST Tangier, Tangier, Morocco

<sup>2</sup> Faculty of science and technics, Ancienne Route de l'Aéroport, Km 10, Ziaten, BP 416, Tangier, Morocco

<sup>3</sup> Universidad de Cadiz Departamento de Física de la Materia Condensada and Instituto de Microscopía Electrónica y materiales (IMEYMAT), Cadiz, Spain

<sup>4</sup> Laboratory of Optoelectronics, Physical Chemistry Materials and Environmental, Department of Physics, Faculty of Sciences, Ibn Tofail University, BP 242, Kenitra, Morocco

<sup>5</sup> Laboratory of Magnetism and High Energies Physics, URAC 12, Department of Physics, Faculty of Science, Mohammed V University-Agdal, B.P. 1014, Rabat, Morocco

structural and optical measurements with the theoretical ab initio calculations by using the first principle.

## 2 Materials and Methods

### 2.1 Experiments Section

The zinc oxide was doped by iron, manganese and chromium and Codoped by cobalt and iron. First the Fedoped ZnO was prepared by mixing 0.3305 g of zinc chloride with a 0.0121 g of iron chloride, corresponding to 5% of iron, and a mass corresponding to 5% percent of chromium chloride, and the same for 5% of Mn. The details were summarized in Tables 1 and 2 for ZnO doped by Fe and Codoped Fe and Co; the same process was made for the others. Then the solutions were sprayed by using a spray pyrolysis on a preheated glass substrate. All the preparation details are tabulated (Tables 1 and 2).

The lattice parameter values for all the samples were closer to the standard values of ZnO lattice parameters. First, we doped ZnO by iron, cobalt, manganese, and chromium. So, the TM atoms replace the sites occupied by zinc at percentages of (5% for Fe and Cr and 5% Fe and 1% Co), The ZnO doped by TM (Fe, Fe/Co, Cr, and Mn) DMS were prepared under  $T = 450$  °C temperature by the spray pyrolysis technique. The XRD patterns for all samples were recorded using x-ray diffractometer with Cu  $K\alpha$  radiation source ( $\lambda = 1.5406$  Å).

The optical properties of the TM (Fe, Fe/Co, Cr, and Mn)-doped ZnO systems, were performed by the UV-spectrophotometer in order to draw the transmission and absorption spectra of these compounds and to study the optical properties and its relations with the doping effects on the ZnO lattice structures, and its relation, generally, with the physical and magnetic properties of each DMS, which could be a multifunction device if it combines between many physical properties.

### 2.2 Calculation Method

For solving the DFT of one-particle equations, we have used multiple-scattering theory: the Korringa–Kohn–Rostoker (KKR)-Green Function, the coherent-potential approximation (KKR-CPA) [34–36] for low concentrated impurity,

**Table 1** Information of sample Fe-doped ZnO

| ZnO mass (g) | Fe mass (g) | Per percentage of Fe (%) | Flow rate (ml/min) | Deposition time (min) |
|--------------|-------------|--------------------------|--------------------|-----------------------|
| 0.3305       | 0.0121      | 5                        | 1.5                | 20                    |

**Table 2** Information sample FeCo-doped ZnO

| ZnO mass (g) | Fe mass (g) | Co mass (g) | Percentage of Fe (%) | Percentage of Co (%) | Flow rate (ml/min) | Deposition time (min) |
|--------------|-------------|-------------|----------------------|----------------------|--------------------|-----------------------|
| 0.3202       | 0.0202      | 0.0032      | 5                    | 1                    | 1.5                | 20                    |

produced by Akai of Osaka University and the Moruzzi, Janack, and the Williams (mjl) parameterization to describe the exchange-correlation energy functional [37, 38]. Throughout these calculations, we based our calculations and simulations on the ZnO wurtzite structure (space group P63mc. The Experimental lattice constants are ( $a = b = 3, 2499$  Å,  $c = 5, 2066$  Å) for ZnO lattice constants, and the internal coordinate is ( $u = 0.345$ ).

## 3 Result and Discussions

### 3.1 X-ray Diffraction

The lattice parameters for each concentrations of Fe, Fe/Co, Cr, and Mn TM, were obtained from the x-ray diffraction (XRD), shown in Fig. 1, by using Formula (1):

$$\frac{1}{a^2} = \frac{4}{3a^2} [h^2 + hk + k^2] + \frac{l^2}{c^2} \quad (1)$$

where  $h$ ,  $k$ , and  $l$  are Miller's indices.

The volume of unit cell was calculated by the using (2) [39]

$$V = \frac{\sqrt{3}}{2} a^2 c \quad (2)$$

The XRD results (Fig. 1) indicated that the  $\text{Co}^{2+}$ ,  $\text{Fe}^{2+}$ ,  $\text{Cr}^{2+}$ ,  $\text{Mn}^{2+}$  TM ions, are incorporated into the ZnO lattice host and replaced  $\text{Zn}^{2+}$  sites by changing the Wurtzite structure volume which gave different interactions between each atoms. Consequently, it gave a change on the electronic, optical, and magnetic properties of ZnO (5% Fe), ZnO (5% Fe and 1% Co), ZnO (5% Cr), and ZnO (5% Mn).

Finally, the XRD parameters was computed, consequently, the ab initio calculation showed different results of electronic and magnetic properties of TM-doped ZnO, impurities.

### 3.2 Optical Measurements

In our case, we are interested on the transmission spectra (Figs. 2 and 3a) in order to class each material and identify which one could be a photo-electrode or a blocking layer in solar cells. From the solid band theory, the relationship between the absorption coefficient  $\alpha$  and the energy of the

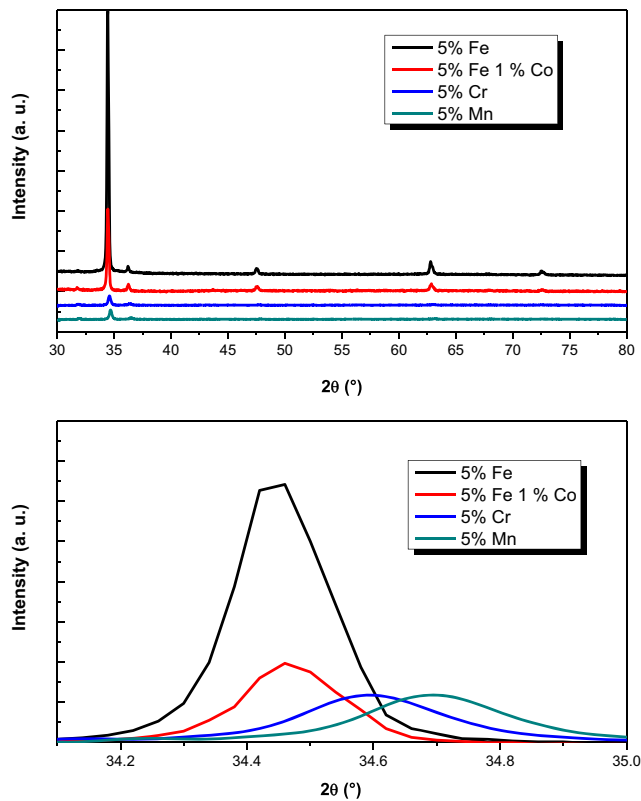


**Fig. 1** Summary of structural and optical parameters in ZnO/TM thin films with different average

incident light  $h\nu$  near the absorption edge of semiconductors is given by the known Tauc's relation for direct band gap:

$$(\alpha h\nu)^2 = A(h\nu - E_g) \tag{3}$$

where  $A$  is a constant and  $E_g$  is the band gap.

The optical band gap energy ( $E_g$ ) was determined from the absorption measurement by analyzing the optical data with the optical coefficient and the photon energy  $h\nu$  using the following equation for direct band gap materials.

The band gap was calculated by the extrapolation of the curves (Fig. 2b) as we have a direct band gap in the case of ZnO. The values of  $E_g$  can be determined by taking the intercept of the extrapolation to zero absorption with photon energy axis  $(\alpha h\nu) \rightarrow 0$  (Fig. 2b).

The optical band gap of the ZnO doped by TM (5% Fe, 5% Fe and 1% Co, 5% Cr), is shown in Fig. 2b.

### 3.3 Magnetic Properties

The ZnO doped by TM (Fe, Co/Fe, Co, and Mn) showed different interactions from the AKAI theoretical calculations, which can explain also the different optical band gaps value;

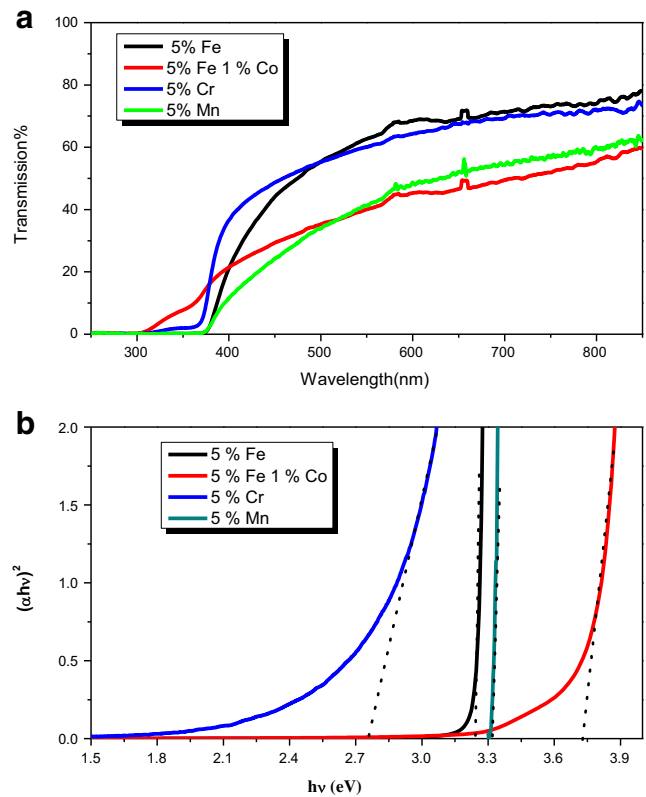


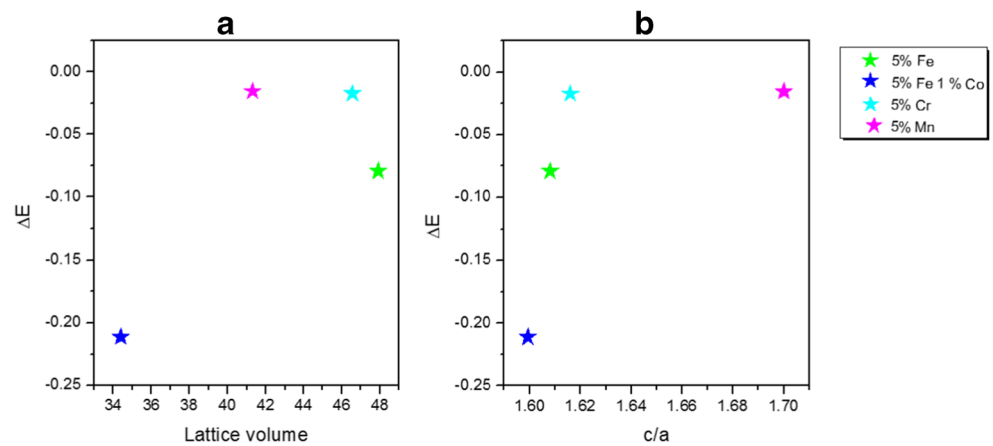
**Fig. 2** a Optical transmission of the ZnO doped by TM (5% Fe, 5% Fe and 1% Co, 5% Cr, and 5% Mn). b Optical band gap of the ZnO doped by TM (5% Fe, 5% Fe and 1% Co, 5% Cr, and 5% Mn)

therefore, the increase or decrease in the value of  $E_g$  for the TM-doped ZnO could be explained by the  $p-d$  double exchange generally due to the hybridization between different  $p$  orbitals of the ZnO host lattice and the  $d$  orbitals of the TM (Fe, Fe/Co, Cr, and Mn). On the other hand, in this study, we tried to explain each results from the interactions phenomena of TM with the host ZnO; consequently, we got different results (Figs. 4, 5, 6, 7, 8, 9, 10, 11; Tables 3, 4, 5) which can help us to give different physical property information and finally propose an application for each device. In our case, we have proved that TM-doped ZnO are ferromagnetic and can be also a good anode in photovoltaic solar cells.

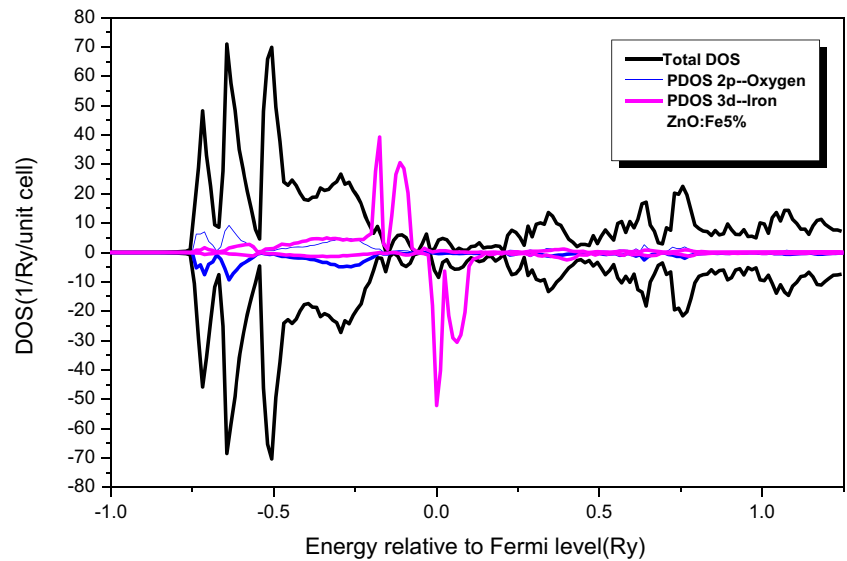
To confirm that the ferromagnetic state is the most dominant, we verified the magnetic stability by a method consisting on calculating system's energy before and after the spin split into two equal parts (one is polarized up and the other is polarized down). The energy in the first case corresponds to the ferromagnetic state, and in the second, a disordered local magnetic (DLM) states.

Comparing these two energies, we can come to the fact that the most stable state of the system (ferro or DLM) has a

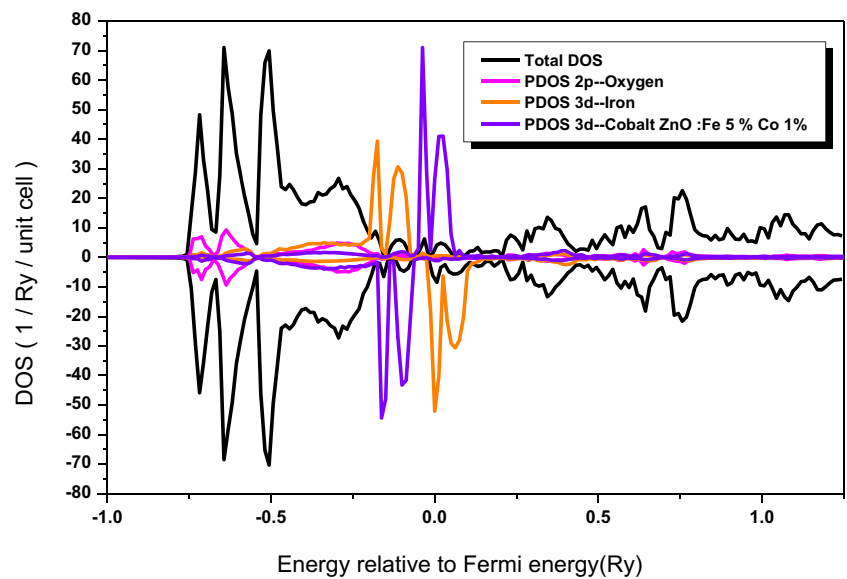
**Fig. 3** **a** Energy difference vs lattice volume **b** Energy difference vs  $c/a$



**Fig. 4** Total and partial density of Fe-doped ZnO semiconductor with explanation of spin up and down densities around Fermi level



**Fig. 5** Total density and partial density of cobalt, iron cobalt, and Co-doped ZnO semiconductor



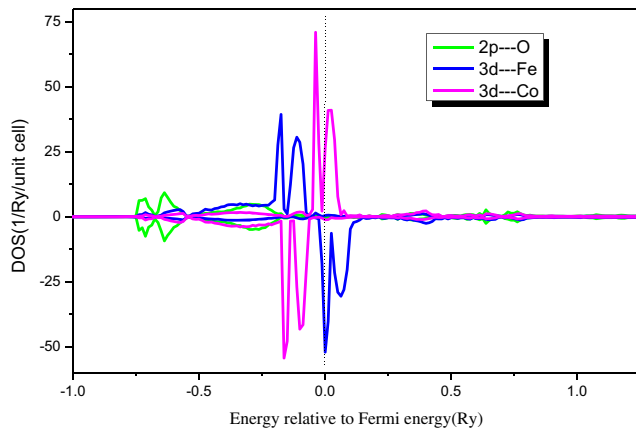


**Fig. 6** Explanations of the hybridization between 2*p*-oxygen and 3*d*-Fe and 3*d*-Co, in FeCo-doped ZnO (5% Fe and 1% Co)

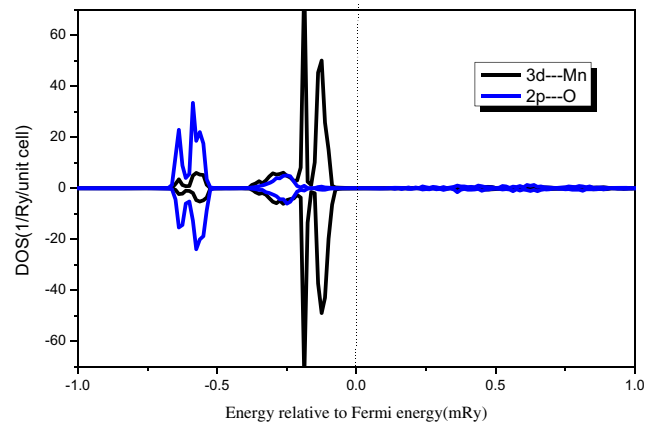


**Fig. 9** Explanations of the hybridization between 2*p*-oxygen and 3*d*-Mn in Mn-doped ZnO

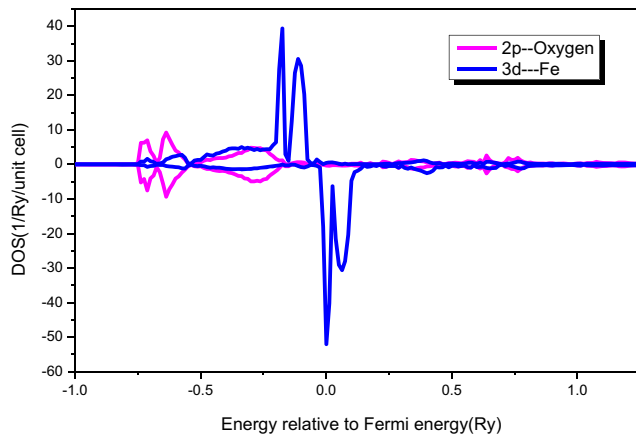


**Fig. 7** Explanations of the hybridization between 2*p*-oxygen and 3*d*-Fe in Fe-doped ZnO

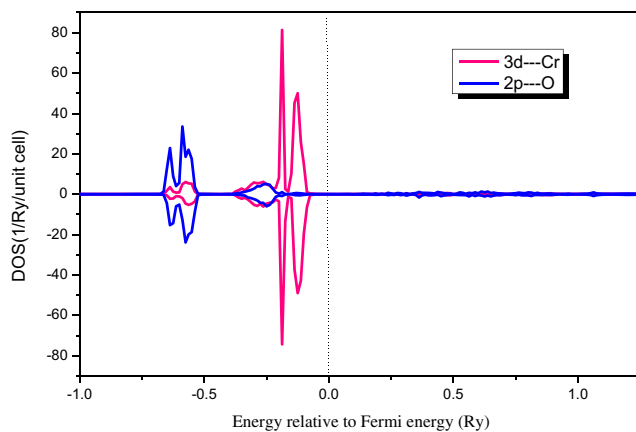


**Fig. 8** Explanations of the hybridization between 2*p*-oxygen and 3*d*-Cr in Fe-doped ZnO

minimum energy. From this calculation, we can also obtain the Curie temperature, by the following equation:

$$K_B T_C = \frac{3 \Delta E}{2 c} \tag{4}$$

$K_B$  = Boltzmann constant.

$T_C$  = Curie temperature.

$\Delta E$  = Energy difference between the DLM and ferromagnetic state.

$c$  = concentration of the dopant element.

In these calculations, this substitutional disorder is performed by using the KKR-CPA method. The total energy difference between the spin-glass states and the ferromagnetic states for DMS in ZnO was calculated by using the local density approximation as a function of 3*d*-TM (Fe, Fe/Co, Cr, and Mn) transition metal impurity.

The total and partial density of Fe-doped ZnO semiconductor with explanation of spin up and down densities around Fermi level, are shown in Fig. 4. The total density

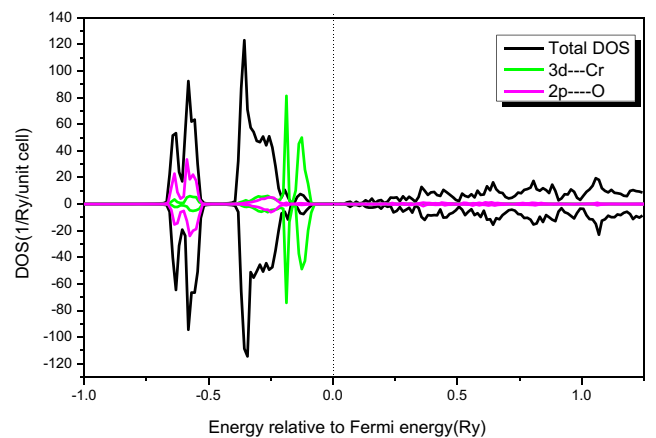


**Fig. 10** Explanations of the hybridization between 2*p*-oxygen and 3*d*-Cr in Cr-doped ZnO and total DOS

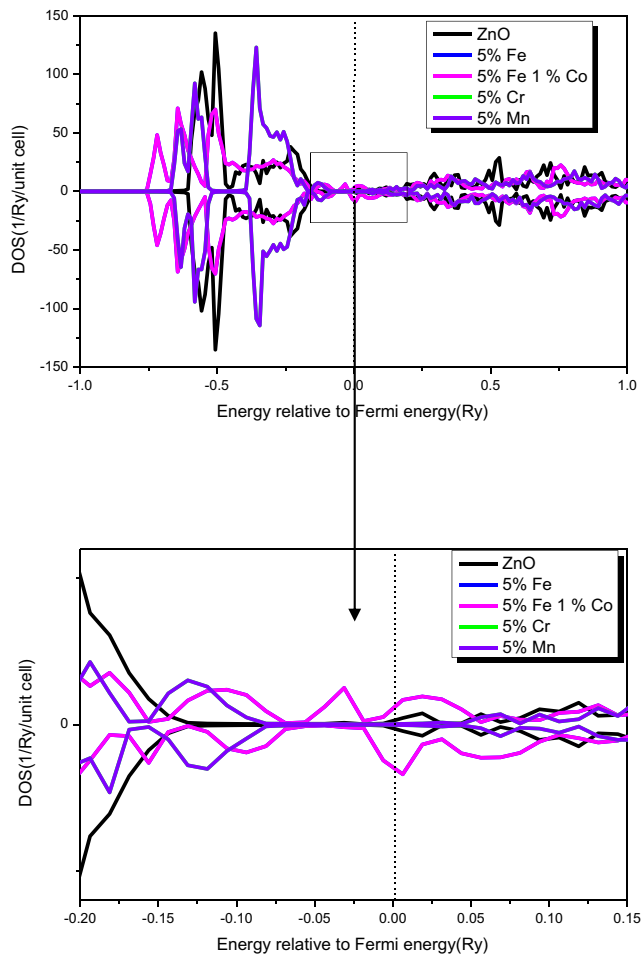


**Fig. 11** Total and partial densities of cobalt, iron cobalt Co-doped ZnO semiconductor

and partial density of cobalt, iron cobalt, Co-doped ZnO semiconductor are shown in Fig. 5.

The explanations of the hybridization between  $2p$ -oxygen and  $3d$ -Fe,  $3d$ -Co, in FeCo-doped ZnO (5% Fe and 1% Co) are shown in Fig. 6. Explanations of the hybridization between  $2p$ -oxygen and  $3d$ -Fe in Fe-doped ZnO are shown in Fig. 7. Explanations of the hybridization between  $2p$ -oxygen and  $3d$ -Cr in Cr-doped ZnO are shown in Fig. 8. Explanations of the hybridization between  $2p$ -oxygen and  $3d$ -Mn in Mn-doped ZnO are shown in Fig. 9. Total density and partial density of cobalt, iron cobalt, and Co-doped

**Table 3** Total energy between the FM and AFM states and temperature Curie of TM ZnO doped

| % of ZnO dopant At 450 °C (SPRAY temperature deposition) | Ferro energy (mRy) | DLM energy (mRy) | Ferro or DLM (mRy) | Tc (K) |
|--|--------------------|------------------|--------------------|--------|
| 5% Fe  | -7366.9371390      | -7366.9370596    | Ferro              | 167.22 |
| 5% Fe and 1% Co  | -7381.0173068      | -7381.0170955    | Ferro              | 420    |
| 5% Cr  | -7322.8372052      | -7322.8371879    | Ferro              | 36.43  |
| 5% Mn  | -7344.4395182      | -7344.4395028    | Ferro              | 32.42  |

**Table 4** Total magnetic moment of different TM (Fe, FeCo, Cr) doped ZnO

| Atomes                              | 5% Fe and 1% Co | ZnO/Fe 5% | ZnO/Cr 5% | ZnO/Mn5% |
|-------------------------------------|-----------------|-----------|-----------|----------|
| Total moment ( $\mu_{\text{tot}}$ ) | 0.6020          | 0.1928    | 0.3574    | 0.4940   |

ZnO are shown in Fig. 10. And for all the TM (5% Fe, 5% Fe and 1% Co, 5% Cr, 5% Mn)-doped ZnO, the band gaps were found to be tuned, giving many information about the materials (Fig. 11).

The decrease of the optical band gaps, is explained by the Zener double exchange of different TM atoms with the oxygen atoms of the host lattice of ZnO and exactly by the hybridization between the  $2p$  oxygen orbitals and  $3d$  TM (Fe, Fe/Co, Cr, and Mn) (Figs. 6, 7, 8, 9), which gave many interactions, and finally, a change in the optical and magnetic properties of each devices (Fig. 11; Tables 4 and 5).

We have calculated the difference in energy between the antiferromagnetic (AFM) and ferromagnetic (FM) configurations. A negative  $\Delta E$  means that the AFM state is more stable than the FM state, and vice versa. In all cases,  $\Delta E$  is found to be negative, as presented in Table 4, confirming that the AFM states are more stable than the FM ones. However, the values of  $\Delta E$  are very small which confirms the competition between the AFM and FM interactions especially in the case of Cr doping. We note that  $\Delta E$  decreases with increasing Fe, Co, and Cr contents and depends also on the nature of the TM atoms, in the case of chromium, the difference energy was found to be very small which explains the competitions between the FM and AFM states, was found to be more important for this TM than for others TM (Table 4).

The total magnetic moment was found to be higher in comparison with other TM-doped ZnO thin films (Table 5) and the Curie temperature was found to be closer to RTFM (Table 4). We can explain that by the decrease of the volume of the lattice due to the exchange interactions of different dopant TM atoms and the oxygen atoms of the host lattice, especially for FeCo (Fig. 3).

**Table 5** Summary of structural, magnetic and optical parameters in ZnO/TM thin films with different average TM doping

|                 | $c$ (Å°) | $a$ (Å°) | E <sub>gap</sub> (eV) | $\Delta E$ (mRy) |
|-----------------|----------|----------|-----------------------|------------------|
| Pure ZnO        | 5.2061   | 3.2488   | 3.30                  | –                |
| 5% Fe           | 5.2524   | 3.2663   | 3.24                  | –0.0794          |
| 5% Fe and 1% Co | 4.68624  | 2.93023  | 3.75                  | –0.2113          |
| 5% Cr           | 5.22     | 3.23     | 2.77                  | –0.0173          |
| 5% Mn           | 5.30     | 3.11     | 3.295                 | –0.0154          |

The difference in the total energy between the FM and AFM states, because the device with the lower energy is the most stable, can explain also the value of  $T_c$ , because the competition between the AFM and the FM ones, is lower, which makes (FeCo)-doped ZnO a good candidate to be an RTFM DMS (Table 4). The summary of structural, magnetic and optical parameters in ZnO/TM thin films with different average TM doping can be found in Tables 4 and 5.

## 4 Conclusion

TM (Fe, Fe/Co, Cr, and Mn)-doped ZnO was deposited by spray pyrolysis technique; the wurtzite structure and the crystallinity were confirmed by XRD; the optical properties and bandgap were investigated from the UV spectrophotometer measurements; and the band structure was studied and confirms the results found by AKAI ab initio calculations; the AFM and FM states were investigated and confirmed the competition of different states (FM and AFM) which are responsible for different properties, magnetic, and optical, which is explained by the different values of the optical band gaps (the experimental) and Curie temperature (calculated). So, the theoretical investigations are in agreement with the experiments and with other research groups. We propose the following design for optical applications and nanospintronics.

**Acknowledgements** This work is supported by the Hassan II Academy of Science and Technology, Integrated Action MA/10/228 and the CNRST-URAC-14, PPR/2015/9-, Morocco.

## References

- Dederichs, P.H., Sato, K., Katayama-Yoshida, H.: Dilute magnetic semiconductors. *Phase Transit.* **78**(9-11), 851–867 (2005)
- Dietl, T.: A ten-year perspective on dilute magnetic semiconductors and oxides. *Nat. Mater.* **9**(12), 965–974 (2010)
- Dietl, T.: Dilute magnetic semiconductors: functional ferromagnets. *Nat. Mater.* **2**(10), 646–648 (2003)
- Coe, J.: Dilute magnetic oxides. *Curr. Opin. Solid State Mater. Sci.* **10**(2), 83–92 (2006)
- Pearson, S., Heo, W., Ivill, M., Norton, D., Steiner, T.: Dilute magnetic semiconducting oxides. *Semicond. Sci. Technol.* **19**(10), R59 (2004)
- Wolf, S., Awschalom, D., Buhrman, R., Daughton, J., Von Molnar, S., Roukes, M., Chtchelkanova, A.Y., Treger, D.: Spintronics: a spin-based electronics vision for the future. *Science* **294**(5546), 1488–1495 (2001)
- MacDonald, A., Schiffer, P., Samarth, N.: Ferromagnetic semiconductors: moving beyond (ga, mn) as. *Nat. Mater.* **4**(3), 195–202 (2005)
- Ohno, H.: Making nonmagnetic semiconductors ferromagnetic. *Science* **281**(5379), 951–956 (1998)
- Ney, A., Opel, M., Kaspar, T.C., Ney, V., Ye, S., Ollefs, K., Kammermeier, T., Bauer, S., Nielsen, K., Goennenwein, S.: Advanced spectroscopic synchrotron techniques to unravel the intrinsic properties of dilute magnetic oxides: the case of co:zno. *New J. Phys.* **12**(1), 013020 (2010)
- Seshadri, R.: Zinc oxide-based diluted magnetic semiconductors. *Curr. Opin. Solid State Mater. Sci.* **9**(1), 1–7 (2005)
- Kittilstved, K.R., Norberg, N.S., Gamelin, D.R.: Chemical manipulation of high- $t_c$  ferromagnetism in zno diluted magnetic semiconductors. *Phys. Rev. Lett.* **94**(14), 147209 (2005)
- Ueda, K., Tabata, H., Kawai, T.: Magnetic and electric properties of transition-metal-doped ZnO films. *Appl. Phys. Lett.* **79**(7), 988–990 (2001)
- Jin, Z., Fukumura, T., Kawasaki, M., Ando, K., Saito, H., Sekiguchi, T., Yoo, Y., Murakami, M., Matsumoto, Y., Hasegawa, T.: High throughput fabrication of transition-metal-doped epitaxial ZnO thin films: a series of oxide-diluted magnetic semiconductors and their properties. *Appl. Phys. Lett.* **78**(24), 3824–3826 (2001)
- Sato, K., Katayama-Yoshida, H.: Stabilization of ferromagnetic states by electron doping in Fe-, Co- or Ni-doped ZnO. *Jpn. J. Appl. Phys.* **40**(4A), L334 (2001)
- Karmakar, D., Mandal, S., Kadam, R., Paulose, P., Rajarajan, A., Nath, T.K., Das, A.K., Dasgupta, I., Das, G.: Ferromagnetism in fe-doped zno nanocrystals: experiment and theory. *Phys. Rev. B* **75**(14), 144404 (2007)
- Liu, H., Yang, J., Zhang, Y., Yang, L., Wei, M., Ding, X.: Structure and magnetic properties of fe-doped zno prepared by the sol-gel method. *J. Phys.: Condens. Matter* **21**(14), 145803 (2009)
- Lee, H.-J., Jeong, S.-Y., Cho, C.R., Park, C.H.: Study of diluted magnetic semiconductor: co-doped ZnO. *Appl. Phys. Lett.* **81**(21), 4020–4022 (2002)
- Gacic, M., Jakob, G., Herbort, C., Adrian, H., Tietze, T., Brück, S., Goering, E.: Magnetism of co-doped zno thin films. *Phys. Rev. B* **75**(20), 205206 (2007)
- Matsumoto, Y., Murakami, M., Shono, T., Hasegawa, T., Fukumura, T., Kawasaki, M., Ahmet, P., Chikyow, T., Koshihara, S.-Y., Koinuma, H.: Room-temperature ferromagnetism in transparent transition metal-doped titanium dioxide. *Science* **291**(5505), 854–856 (2001)
- Saeki, H., Tabata, H., Kawai, T.: Magnetic and electric properties of vanadium doped ZnO films. *Solid State Commun.* **120**(11), 439–443 (2001)
- Liu, C., Yun, F., Morkoc, H.: Ferromagnetism of ZnO and GaN: a review. *J. Mater. Sci. Mater. Electron.* **16**(9), 555 (2005)
- Park, J.H., Kim, M.G., Jang, H.M., Ryu, S., Kim, Y.M.: Co-metal clustering as the origin of ferromagnetism in Co-doped ZnO thin films. *Appl. Phys. Lett.* **84**(8), 1338–1340 (2004)
- Liu, Y., Yang, Y., Yang, J., Guan, Q., Liu, H., Yang, L., Zhang, Y., Wang, Y., Wei, M., Liu, X.: Intrinsic ferromagnetic properties in Cr-doped ZnO diluted magnetic semiconductors. *J. Solid State Chem.* **184**(5), 1273–1278 (2011)
- Yılmaz, S., Parlak, M., Özcan, Ş., Altunbaş, M., McGlynn, E., Bacakşz, E.: Structural, optical and magnetic properties of Cr

- doped ZnO microrods prepared by spray pyrolysis method. *Appl. Surf. Sci.* **257**(22), 9293–9298 (2011)
25. Roberts, B.K., Pakhomov, A.B., Shutthanandan, V.S., Krishnan, K.M.: Ferromagnetic Cr-doped ZnO for spin electronics via magnetron sputtering. *J. Appl. Phys.* **97**(10), 10D310 (2005)
  26. Sharma, P., Gupta, A., Rao, K., Owens, F.J., Sharma, R., Ahuja, R., Guillen, J.O., Johansson, B., Gehring, G.: Ferromagnetism above room temperature in bulk and transparent thin films of Mn-doped ZnO. *Nat. Mater.* **2**(10), 673–677 (2003)
  27. Fukumura, T., Jin, Z., Ohtomo, A., Koinuma, H., Kawasaki, M.: An oxide-diluted magnetic semiconductor: Mn-doped ZnO. *Appl. Phys. Lett.* **75**(21), 3366–3368 (1999)
  28. Wang, X.L., Luan, C.Y., Shao, Q., Pruna, A., Leung, C.W., Lortz, R., Zapien, J.A., Ruotolo, A.: Effect of the magnetic order on the room-temperature band-gap of mn-doped zno thin films. *Appl. Phys. Lett.* **102**(10), 102112 (2013)
  29. Özgür, Ü., Alivov, Y.I., Liu, C., Teke, A., Reshchikov, M., Doğan, S., Avrutin, V., Cho, S.-J., Morkoc, H.: A comprehensive review of ZnO materials and devices. *J. Appl. Phys.* **98**(4), 11 (2005)
  30. Srikant, V., Clarke, D.R.: On the optical band gap of zinc oxide. *J. Appl. Phys.* **83**(10), 5447–5451 (1998)
  31. Pearton, S.J., Norton, D.P., Ivill, M.P., Hebard, A.F., Zavada, J.M., Chen, W.M., Buyanova, I.A.: ZnO doped with transition metal ions. *IEEE Trans. Electron. Devices* **54**(5), 1040–1048 (2007)
  32. Fukumura, T., Yamada, Y., Toyosaki, H., Hasegawa, T., Koinuma, H., Kawasaki, M.: Exploration of oxide-based diluted magnetic semiconductors toward transparent spintronics. *Appl. Surf. Sci.* **223**(1), 62–67 (2004)
  33. Fukumura, T., Toyosaki, H., Yamada, Y.: Magnetic oxide semiconductors. *Semicond. Sci. Technol.* **20**(4), S103 (2005)
  34. Katayama, H., Terakura, K., Kanamori, J.: Hyperfine field of positive muon in ferromagnetic nickel. *Solid State Commun.* **29**(5), 431–434 (1979). doi:[10.1016/0038-1098\(79\)91210-9](https://doi.org/10.1016/0038-1098(79)91210-9)
  35. Blügel, S., Akai, H., Zeller, R., Dederichs, P.: Hyperfine fields of 3d and 4d impurities in nickel. *Phys. Rev. B* **35**(7), 3271 (1987)
  36. Akai, H.: Fast Korringa-Kohn-Rostoker coherent potential approximation and its application to FCC Ni-Fe systems. *J. Phys. Condens. Matter* **1**(43), 8045–8064 (1989). doi:[10.1088/0953-8984/1/43/006](https://doi.org/10.1088/0953-8984/1/43/006)
  37. Aoki, H., Akai, H., Hosaka, A., Toki, H., Malik, F.: *Condensed Matter Theories*, vol. 21. Nova Science, Tokyo (2007)
  38. Akai, H.: KKR-CPA Program package
  39. Zak, A.K., Majid, W.A., Abrishami, M.E., Yousefi, R.: X-ray analysis of ZnO nanoparticles by Williamson–Hall and size–strain plot methods. *Solid State Sci.* **13**(1), 251–256 (2011)